Strain-less directed self-assembly of Si nanocrystals on patterned SiO_2 substrate

Jingjian Ren,[1] Hao Hu,[2] Feng Liu,[2] Sheng Chu,[1] and Jianlin Liu[1,a)]
[1]*Quantum Structures Laboratory, Department of Electrical Engineering, University of California, Riverside, California 92521, USA*
[2]*Department of Materials Science and Engineering, University of Utah, Salt Lake City, Utah 84112, USA*

(Received 1 May 2012; accepted 31 July 2012; published online 6 September 2012)

Strain induced self-assembled Stranski-Krastanov growth of semiconductor islands on patterned substrate has shown great improvement of island size uniformity and spatial order. Here, we show self-assembled Volmer-Weber (V-W) growth of Si nanocrystals (NCs) on patterned SiO_2 substrate via traditional chemical vapor deposition method under certain experimental configurations, induced by surface/interface energy competition without strain. A simplified two-dimensional theoretical model is developed to elucidate V-W island nucleation on the pattern substrate with varied morphologies, which shows good consistency with the experimental results. Our studies provide a general guidance for directing the growth and self-assembly of NCs on non-planar oxide substrates. © *2012 American Institute of Physics*. [http://dx.doi.org/10.1063/1.4749269]

INTRODUCTION

As electronic devices scale down, it becomes more and more technically challenging to continue miniaturization of semiconductor nanostructures relying on lithography only. Alternatively, self-assembly is of significant interest to both academic research and industrial applications due to the potential of getting ordered nanostructures at ultra-scaled regime. Both experimental and theoretical efforts have been invested extensively into study of growth of group III-V and group IV quantum dots (QDs) or islands on single-crystalline substrates,[1–5] aiming at exploring predictable and well-controlled QD growth with supreme spatial uniformity and understanding the underlying physical mechanism. Perfect self-alignment of Ge QDs on Si ridge,[6–10] SiGe QDs on lithographically patterned Si substrate,[11] and InAs QDs on GaAs plateau[12,13] were reported by many groups, and different models were built to address the directed nucleation effect of strained islands.[10,11,14,15]

Mediated by a substrate morphology induced strain relaxation mechanism, so far, most practices of directed self-assembly of islands have been towards strained islands on patterned substrates. However, unstrained islands growth on amorphous substrate such as SiO_2 is also of great importance because of modern electronic device demands. Among many applications, one example is metal-oxide-semiconductor structure based nanocrystal floating gate memories,[16] which require high-density ultra-uniform metallic or semiconductor NCs on oxide surface to circumvent device performance variability issue. Thus, identifying a growth mechanism that will lead to a "strain-less" directed self-assembly of NCs in V-W mode on oxide substrates is of both scientific interest and technological significance. One intriguing question is how NCs grow on patterned oxide substrate and whether the non-planar surface morphology can direct NCs self-assembly in the absence of strain.

In this work, we present our experimental observations of preferential nucleation and growth of Si NCs on patterned SiO_2 substrate, showing direct evidence of strain-less directed self-assembly. The growth condition dependence of this preferential growth effect is studied. A simple two-dimensional (2D) model is developed and calculation is performed in terms of the energetics associated with V-W island growth on the patterned substrate, to explain these interesting experimental findings.

EXPERIMENTAL RESULTS

Substrates for Si NCs growth were prepared as follows. E-beam lithography was employed to pattern the resist on pre-cleaned p-type Si (100) substrates. Cr was evaporated in a high-vacuum e-beam evaporation system. This was followed by a lift-off process to form hard-mask as shown in the schematic in Fig. 1(a) for subsequent wet etching step. KOH anisotropic wet etching was performed on the samples and well-defined pit-shaped patterns were achieved. After organic contaminants and metal residue cleaning and native oxide removal, samples were immediately transferred into an oxide furnace for dry oxidation. 5 nm thermal oxide on the surface of the pit-shaped substrates was formed at 950 °C with clean and flat surface, as one pit shown in the scanning electron microscopy (SEM) image in Fig. 1(b).

Chemical vapor Si NCs deposition technology has been explored and developed for NC memory applications, and silicon crystallites with nanometer size can be reliably obtained by controlling the early stages of Si film growth.[16–19] In our experiments, Si NCs growth was performed on the patterned substrates in a low pressure chemical vapor deposition (LPCVD) system with split growth conditions. During the growth, SiH_4 was used as Si precursor and the flow rate was fixed at SiH_4:N_2 = 20 sccm:100 sccm and pressure at 0.5 Torr for all the samples. Growth temperature and growth

a)Author to whom correspondence should be addressed. Electronic mail: jianlin@ee.ucr.edu.

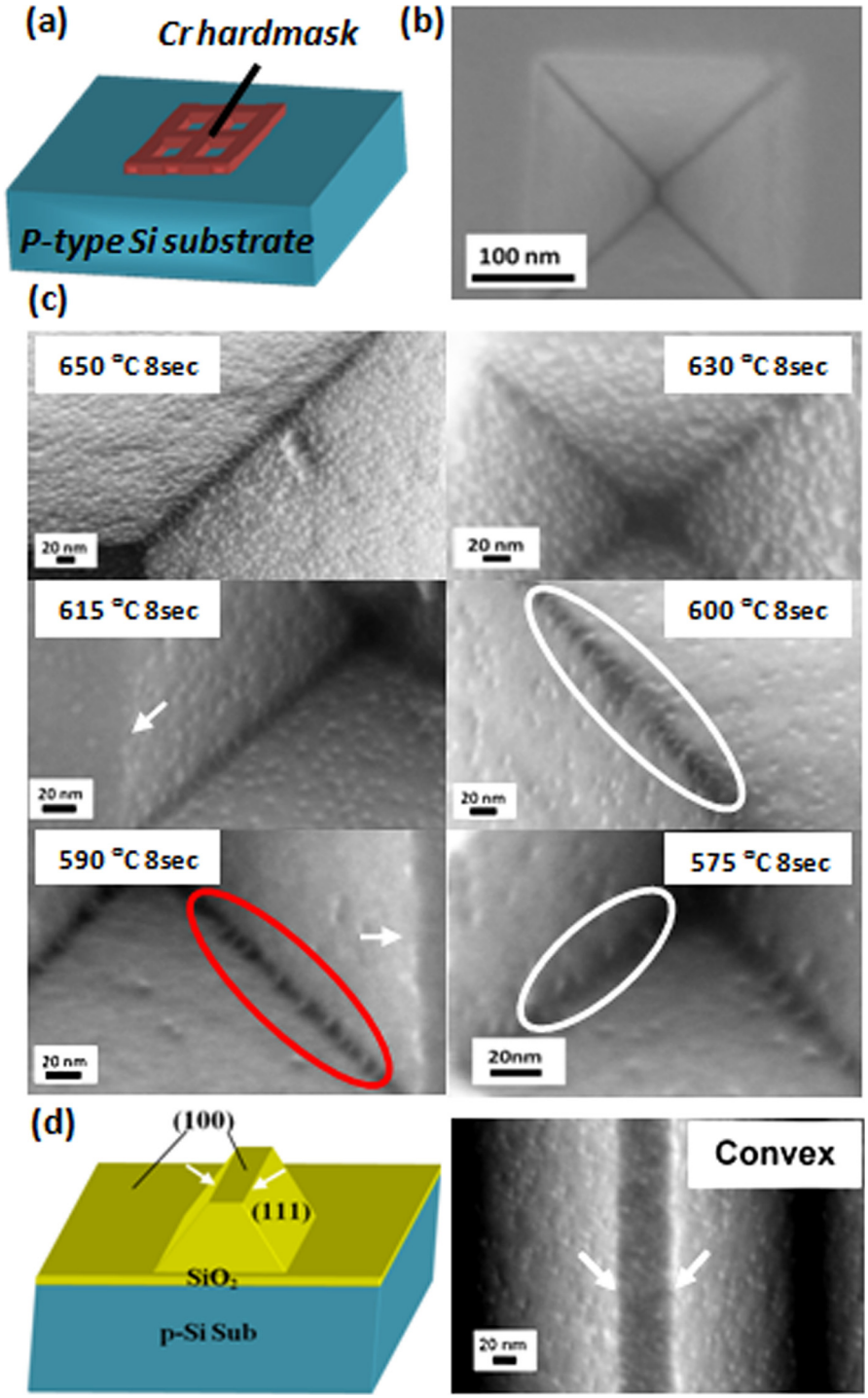

FIG. 1. (a) Schematic of wet etching hardmask for substrate patterning; (b) SEM image of well-defined pit-shaped oxide substrate pattern with clean and flat surface before growth; (c) SEM images of temperature-dependent Si NCs nucleation and growth; and (d) schematic of convex oxide substrate and SEM image of Si NCs growth on this type of substrate.

time were chosen as the parameters to be tuned for condition split study of nucleation and growth behavior of NCs. Temperature is believed to be directly related to the energy gained by adatoms during growth, which is critical in determining the migration behavior and nucleation barrier. Different growth time shows the evolvement of Si dots nucleation and growth and allows one to see a clear picture of NC growth process during different stages.

Fig. 1(c) shows SEM images of temperature-dependent Si NCs nucleation and growth behavior. Samples were grown under six different temperatures from 650 °C to 575 °C with the same growth time of 8 s. To monitor temperature effect on the early stage nucleation and growth behavior of NCs, short growth time was used and NCs with very small sizes were synthesized. Despite the tiny size of NCs (5–10 nm), SEM was able to capture the morphology of NCs after growth and qualitatively show the segregation and NC density variation. From high temperature to low temperature, a clear trend of dot density and size decreasing is observed. Interestingly, while under higher temperatures of 650 °C, 630 °C, and 615 °C, no obvious dot density variation between the wall (planar area) and the trench (concave area) is found, and dot segregation in the trench is observed for lower-temperature samples at 600 °C, 590 °C, and 575 °C, with more NCs gathering in this concave part of the substrate than in other parts. This phenomenon is attributed to the

preferential nucleation of NCs in the trench due to lower NC formation energy induced primarily by the substrate morphology. The fact of the enhanced stress of oxide substrate in this part making the chemical bonds here more reactive for nucleation also contributes to this effect.[19,20] In the particular temperature range of 575 °C–600 °C, adatoms adsorbed to the sample surface move around and find most energy-favorable sites (the concave parts of the substrate) to settle down as nuclei for later NC growth. Afterwards, more adatoms segregate to the nuclei and NCs preferentially form in the trench. Among the three temperatures, 590 °C is the one under which the best preference occurs, with NCs selectively aligned along the trench and almost no dots found on other area outside the trench. This can be considered a consequence of the competition between adatoms surface migration and reaction with substrate atoms (nucleation). At lower temperature of 575 °C, some NCs form on the planar surface due to insufficient energy gained by the adatoms at lower temperatures and the limited migration. Similarly, for samples grown at temperatures below 575 °C, although low NC formation energy locations (trenches) are available, the energy supplied to adatoms is not enough for them to overcome migration barrier and reach the energy-favorable sites. Therefore, no directed self-assembly behavior was found. On the other hand, at higher temperature of 600 °C, the nucleation and growth process are accelerated. Si NC deposition rate is so high that later-stage random nucleation starts covering the directed self-assembly effect at earlier stage. This is intuitive because as earlier-formed NCs fill in the trench, low-energy sites for nucleation are occupied and the effect of substrate morphology on the nucleation and growth of NCs becomes weaker and weaker. Preferential nucleation is then replaced by continuous random NCs deposition on the whole sample surface at later stage with no or a small limitation in the number of nucleation sites.[21] This situation is more pronounced for even higher temperatures, as mentioned above, where almost no sign of preference can be observed from the images. In fact, it is expected that even on samples where directed self-assembly is observed, with longer growth time, this effect would eventually be covered by subsequent random NC formation. This is confirmed by the time-dependent growth experiments in this work. It should also be mentioned that a series of NCs growth with split conditions was also carried out on substrate with plateau as shown in the schematic of Fig. 1(d). Similar directed self-assembly was not observed at either convex parts (i.e., the intersection of (111) and (100) planes as marked by the white arrows) or planar parts of the substrates in our experiments. SEM image in Fig. 1(d) shows a typical sample grown at 600 °C for 30 s.

The growth time dependence of Si NCs deposition on patterned concave substrate surface is shown in Fig. 2. These SEM images present clear surface evolvement of NC samples with growth time at three temperatures (575 °C, 590 °C,

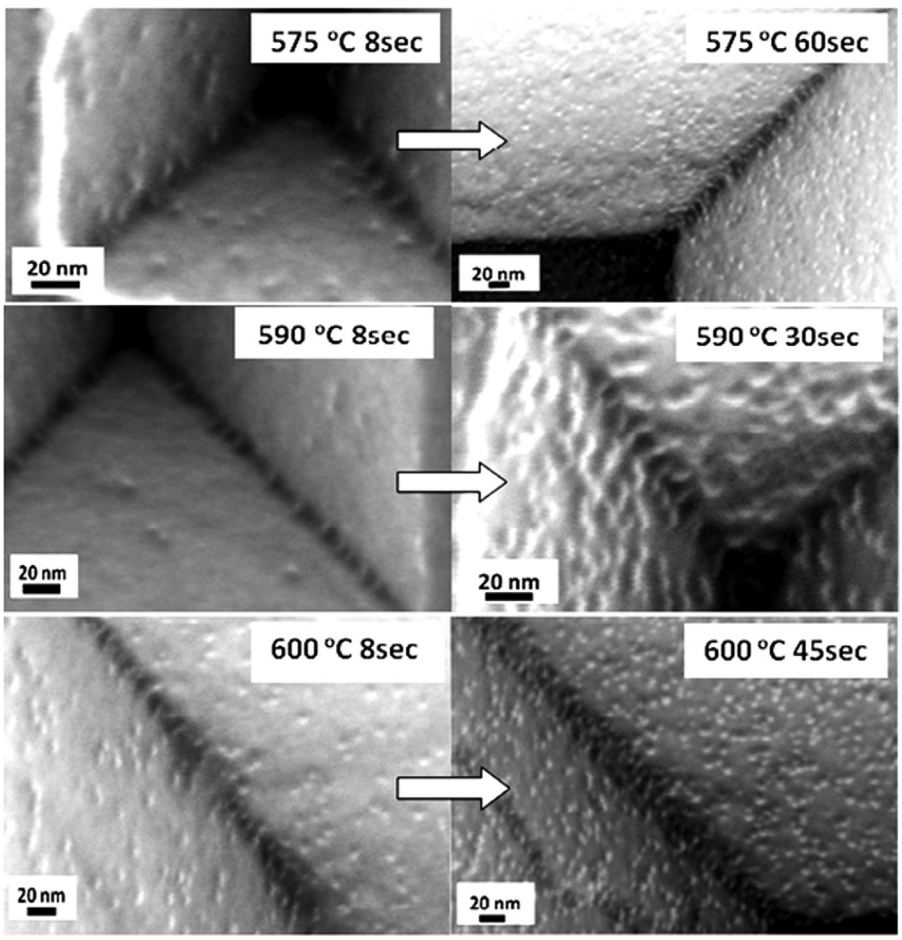

FIG. 2. SEM images of the growth time dependence of Si NCs growth on patterned substrate surface to show the evolvement of NC deposition process at different stages.

and 600 °C). At the initial stage (with growth time of 8 s), three samples show different levels of directed self-assembly. As growth time increases, an increase of dot density and size is noticeable and directed NC formation is covered with dots showing up at locations other than the concave trench. In line with the discussion above, this is because of the occupation of energy-favorable nucleation sites by NCs that offsets the morphology-induced NC formation energy difference among concave, flat, and convex areas.

The growth condition splits for all the samples are summarized in Fig. 3, with X-axis standing for growth temperatures and Y-axis representing growth times. As highlighted in red, the temperature range of 575 °C–600 °C is found to be a temperature window allowing for observation of directed Si NC self-assembly on concave substrate surface, under the given experimental configurations. In other words, samples with oxide thickness of 5 nm grown under pressure of 0.5 Torr and precursor flux of SiH_4:N_2 = 20 sccm:100 sccm show preferential nucleation behavior at these temperatures using growth duration of 8 s. This window could vary with oxide thickness, pressure, and gas source flux. Note that although from an energy point of view, higher temperatures provide adatoms with higher energy to migrate on substrate and promote directed self-assembly, the whole nucleation and growth process occur much faster, leading to difficulty in capturing the effect of interest at earlier stage. Growth conditions need to be tuned carefully in order to reveal this behavior.

MODELING

Different from previously reported self-alignment of semiconductor islands (Ge on Si, InAs on GaAs, etc.), in this case of NC growth on amorphous substrate (e.g., Si NC on SiO_2), another growth mode, i.e., Volmer-Weber (V-W) mode, is involved, in which no wetting of the substrate happens and NC (3D island) nucleation and growth happen from the very beginning. To formulate the theory of NC nucleation on non-planar substrate in this mode, we first consider a 2D model of the NC-patterned substrate system. As shown in Fig. 4(a), this model consists of saw tooth-shaped substrate (thin thermal SiO_2 layer on top of patterned Si substrate) and NCs with constant size (area). The shape of NC is assumed as surface-faceted for simplicity. Three different types of substrate surface morphology are configured, namely, planar, convex, and concave, with substrate angle $\varphi = 0, \varphi > 0, \varphi < 0$, respectively. θ denotes the surface angle of NC and $2l$ is the width of the NC covering the substrate. In this model, surface and interface energy are considered to be dominant factors in determining NC nucleation and no strain relaxation energy term is introduced in the calculation.[23,24] In addition, since this growth mode normally involves material growth on foreign substrate, an interface energy term is included into the total surface energy change of the system. Consequently, the total NC formation energy can be written as

$$\begin{aligned} E_{surf} &= E_{surf-NC} + E_{int} - E_{surf-sub} \\ &= 2l\gamma_{NC}\left(\sec\theta + \frac{\gamma_{int}-\gamma_{sub}}{\gamma_{NC}}\sec\varphi\right) \\ &= 2\gamma_{NC}\left(\sec\theta + \frac{\gamma_{int}-\gamma_{sub}}{\gamma_{NC}}\sec\varphi\right) S^{1/2}(\tan\theta - \tan\varphi)^{-1/2}, \end{aligned} \tag{1}$$

where $E_{surf\text{-}NC}$ is the surface energy of the NC, E_{int} is the interface energy of the interface between the two materials, and $E_{surf\text{-}sub}$ is the surface energy of the substrate covered by NC; $\gamma_{NC}, \gamma_{int}, \gamma_{sub}$ are the surface energy density of NC, interface, and substrate, respectively; and S is the NC area in 2D model.

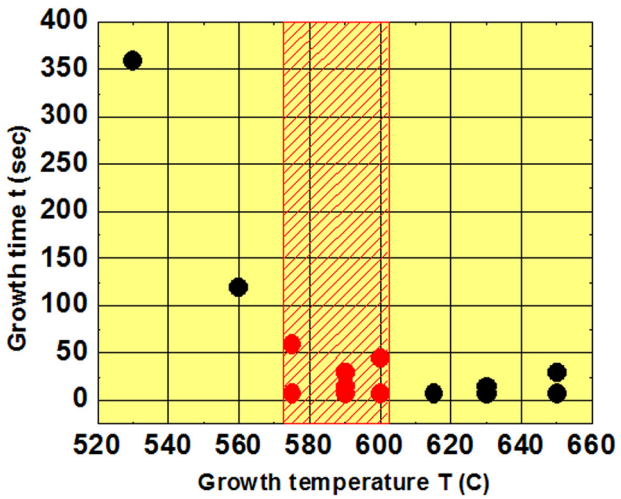

FIG. 3. Summary of growth condition splits and the temperature window for Si NCs preferential growth on concave oxide substrate surface with t_{ox} = 5 nm (temperature window: T = 575 °C–600 °C; gas pressure P = 0.5 Torr, gas flux = SiH_4 20 sccm:N_2 100 sccm).

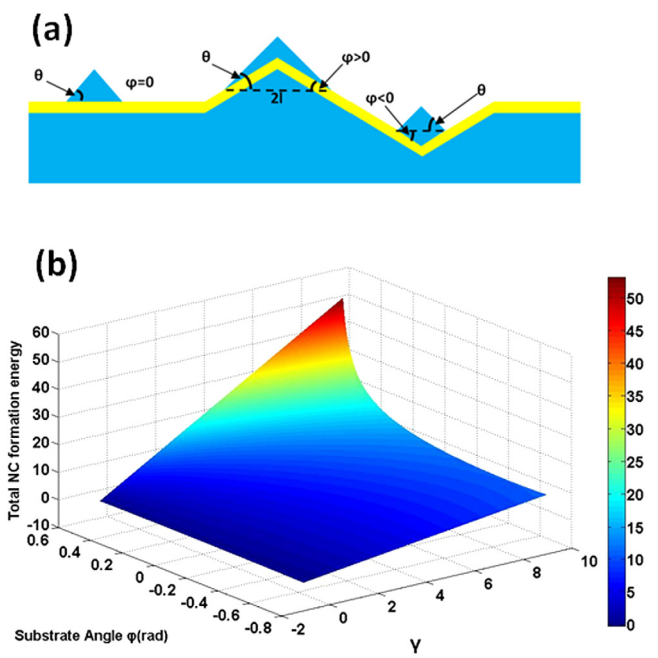

FIG. 4. (a) Two-dimensional model of NC-patterned oxide substrate system; (b) 3-D plot of total NC formation energy as a function of substrate angle φ and system parameter γ, with the unit of energy $2\gamma_{NC}S^{1/2}$.

From Eq. (1), it can be seen that for fixed S and θ, the total NC formation energy is a function of the non-dimensional system parameter $\gamma = \frac{\gamma_{int}-\gamma_{sub}}{\gamma_{NC}}$ and substrate angle φ. To reveal how total NC formation energy varies with different substrate morphologies and γ value, we examined the dependence of E_{surf} on φ and γ with θ fixed at 30° as an example, as shown in Fig. 4(b). In general, the surface contact angle of QD (θ) can have a size dependence even in V-W mode due to edge effect as shown by previous theory[22] and experiments.[21] Here the value is chosen as a representative case just to show the overall trend of the effect of substrate morphology on NC nucleation behavior. γ is an intrinsic parameter related to the nature of the two materials in the system and in different growth modes it holds different value ranges. In V-W mode, $\gamma_{NC}+\gamma_{int} > \gamma_{sub}$ or $\gamma > -1$ is satisfied. Substrate angle φ is investigated within the range $-45° < \varphi \leq 28°$ to meet the restriction that $\varphi \leq \theta$. From the 3-D plot, it should be noticed that E_{surf} increases with the value of γ, qualitatively indicating the fact that the larger this system parameter is, the higher NC formation energy is hence the harder it is for NC to form. Under different γ, the changing trend of E_{surf} with φ varies. In most cases, E_{surf} decreases monotonously with φ decreasing from positive regime to negative regime, suggesting that lower NC formation energy is needed for negative substrate angle (concave) compared to zero (flat) and positive (convex) substrate angle.

To further address the experimental results observed and illustrate the morphology effect, E_{surf} as a function of γ is plotted for the three types of substrate angles for comparison. Fig. 5(a) shows a schematic of the patterned substrate surface utilized in the experimental part to study NC growth behavior, with $\varphi = -35.26°$ at the concave trench of the pit, $\varphi = 0$ on the planar surface, and $\varphi = 27.37°$ at the convex edge of the pit. It can be clearly seen from Fig. 5(b) that within the whole range of variable γ, concave substrate requires lowest NC formation energy than that for the other two cases. This result implies that concave substrate always favors the nucleation and growth of NC in V-W mode, an effect regardless of what material system is involved (γ) and this is in very good consistency with the experimental findings above. While over a large range of γ, lower energy is needed in flat case than that in convex case, the magnified region of the plots in the figure shows that in certain systems, the situation could be reversed, indicating a dramatic dependence of NC formation energy on material natures and interface structures. There have been experimental reports showing NC self-alignment on convex oxide surface with very fine alignment condition window,[25] a proof of more energy-favored nucleation sites on convex surface over flat surface in some systems. It is worth mentioning that the simplified 2D model developed here is aimed at semi-quantitatively describing and explaining the experimental findings, focusing on the directed self-assembly behavior observed on concave surface. The range of γ shown in Fig. 5, (−1, 10), is chosen mainly for illustration of this concave surface effect. Although the specific value of γ could not be obtained due to the amorphous nature of thermal SiO_2 and the unknown interface atomic structure of Si-SiO_2, these calculation results provide direct theoretical evidence to well support and address the experimental findings within the scope of this work.

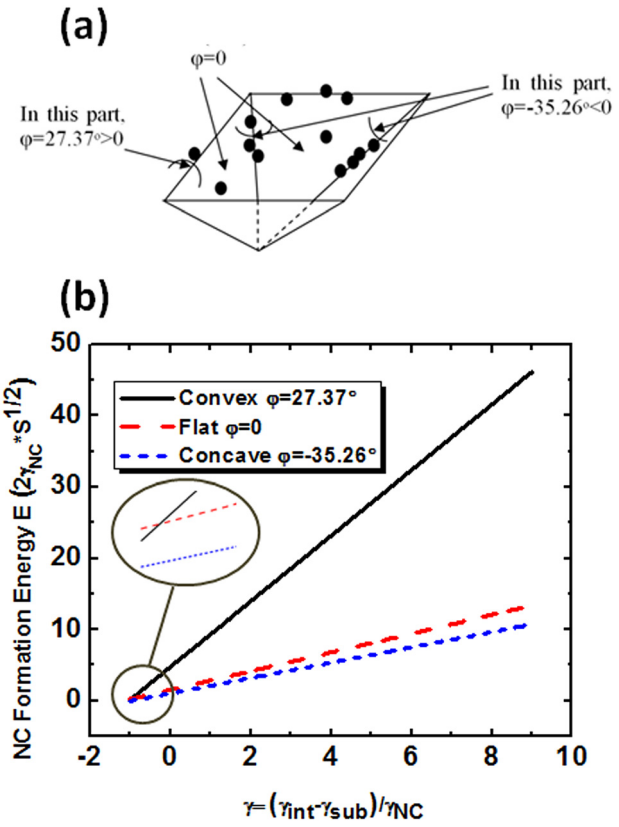

FIG. 5. (a) Schematic of the patterned substrate surface; (b) Calculated total NC formation energy for three different types of experimental surface morphologies.

Previous theory analysis[15] has shown that strain relaxation can favor nucleation of "strained" islands at the concave region on patterned substrates in Stranski-Krastanov (S-K) growth mode. In this study, we show that the competition between surface/interface energy without strain relaxation can also favor nucleation of "unstrained" NCs at the concave region on patterned substrates in V-W growth mode. It is also interesting to note that although the "unstrained" V-W islands have no misfit epitaxial strain, they may still experience stress effects due to surface stress discontinuity at island edges as shown before,[22,26] an effect deserves further study.

CONCLUSION

Preferential growth behavior of Si NCs on patterned SiO_2 substrate was found within certain experimental condition window. Simple modeling and calculation were carried out to depict the possible dominant mechanism underlying the experimental results. Different from common strain energy directed island nucleation on patterned substrate in S-K mode, the surface/interface energy directed NCs growth on amorphous thermal oxide substrate in V-W mode is relatively a weaker effect, which requires the growth parameters to be tuned more strictly for the effect to show up. This work furthers our fundamental understanding of NC

growth behavior on amorphous substrate with various morphologies.

ACKNOWLEDGMENTS

This material is based on research sponsored by DARPA/Defense Microelectronics Activity (DMEA) under Agreement No. H94003-10-2-1003 and the National Science Foundation (NSF) DMR-0807232. The work at Utah is supported by DOE-BES (Grant No. DE-FG02-04ER46148).

[1]S. Yu Shiryaev, F. Jensen, J. Lundsgaard Hansen, J. Wulff Petersen, and A. Nylandsted Larsen, Phys. Rev. Lett. **78**, 503 (1997).
[2]Y. Suda, S. Kaechi, D. Kitayama, and T. Yoshizawa, Thin Solid Films **464–465**, 190 (2004).
[3]D. Kitayama, T. Yoshizawa, and Y. Suda, Jpn. J. Appl. Phys., Part 1 **43**(6B), 3822 (2004).
[4]O. Guise, J. T. Yates, J. Levy, J. Ahner, V. Vaithyanathan, and D. G. Schlom, Appl. Phys. Lett. **87**, 171902 (2005).
[5]S.-S. Ferng, T.-H. Yang, G. Luo, K.-M. Yang, M.-F. Hsieh, and D.-S. Lin, Nanotechnology **17**, 5207 (2006).
[6]T. I. Kamins and R. S. Williams, Appl. Phys. Lett. **71**, 1201 (1997).
[7]G. Jin, J. L. Liu, S. G. Thomas, Y. H. Luo, K. L. Wang, and B.-Y. Nguyen, Appl. Phys. Lett. **75**, 2752 (1999).
[8]Z. Y. Zhong, A. Halilovic, T. Fromherz, F. Schäffler, and G. Bauer, Appl. Phys. Lett. **82**, 4779 (2003).
[9]Z. Y. Zhong, A. Halilovic, M. Mühlberger, F. Schäffler, and G. Bauer, J. Appl. Phys. **93**, 6258 (2003).
[10]B. Yang, F. Liu, and M. G. Lagally, Phys. Rev. Lett. **92**, 025502 (2004).
[11]Z. Y. Zhong, W. Schwinger, F. Schäffler, G. Bauer, G. Vastola, F. Montalenti, and L. Miglio, Phys. Rev. Lett. **98**, 176102 (2007).
[12]R. Zhang, R. Tsui, K. Shiralagi, D. Convey, and H. Goronkin, Appl. Phys. Lett. **73**, 505 (1998).
[13]H. Lee, J. A. Johnson, M. Y. He, J. S. Speck, and P. M. Petroff, Appl. Phys. Lett. **78**, 105 (2001).
[14]G. Katsaros, J. Tersoff, M. Stoffel, A. Rastelli, P. Acosta-Diaz, G. S. Kar, G. Costantini, O. G. Schmidt, and K. Kern, Phys. Rev. Lett. **101**, 096103 (2008).
[15]H. Hu, H. J. Gao, and F. Liu, Phys. Rev. Lett. **101**, 216102 (2008).
[16]S. Tiwari, F. Rana, H. Hanafi, A. Hartstein, E. F. Crabbe, and K. Chan, Appl. Phys. Lett. **68**, 1377 (1996).
[17]S. Miyazaki, Y. Hamamoto, E. Yoshida, M. Ikeda, and M. Hirose, Thin Solid Films **369**, 55–59 (2000).
[18]S. Jacob, B. De Salvo, L. Perniola, G. Festes, S. Bodnar, R. Coppard, J. F. Thiery, T. Pate-Cazal, C. Bongiorno, S. Lombardo, J. Dufourcq, E. Jalaguier, T. Pedron, F. Boulanger, and S. Deleonibus, Solid-State Electron. **52**, 1452–1459 (2008).
[19]F. Mazen, T. Baron, G. Brémond, N. Buffet, N. Rochat, P. Mur, and M. N. Séméria, J. Electrochem. Soc. **150**, G203 (2003).
[20]D. B. Kao, J. P. McVittie, W. D. Nix, and K. C. Saraswat, IEEE Trans. Electron Devices **34**, 1008 (1987).
[21]G. Nicotra, R. A. Puglisi, S. Lombardo, C. Spinella, M. Vulpio, G. Ammendola, M. Bileci, and C. Gerardi, J. Appl. Phys. **95**, 2049 (2004).
[22]F. Liu, Phys. Rev. Lett. **89**, 246105 (2002).
[23]V. M. Kaganer, B. Jenichen, R. Shayduk, W. Braun, and H. Riechert, Phys. Rev. Lett. **102**, 016103 (2009).
[24]L. B. Freund and S. Suresh, *Thin Film Materials-Stress, Defect Formation and Surface Evolution* (Cambridge University Press, 2004), pp. 27–33.
[25]M. Olmedo, A. A. Martinez-Morales, G. Liu, E. Yengel, C. S. Ozkan, C. Ning Lau, M. Ozkan, and J. Liu, Appl. Phys. Lett. **94**, 123109 (2009).
[26]V. A. Shchukin, N. N. Ledentsov, P. S. Kop'ev, and D. Bimberg, Phys. Rev. Lett. **75**, 2968 (1995).